Article

Polyamines play a critical role in the control of the innate immune response in the mouse central nervous system

Denis Soulet and Serge Rivest

Laboratory of Molecular Endocrinology, CHUL Research Center and Department of Anatomy and Physiology, Faculty of Medicine, Laval University, Quebec, Canada G1V 4G2

The present work investigated whether polyamines play a role in the control of the innate immune response in the brain. The first evidence that these molecules may be involved in such a process was based on the robust increase in the expression of the first and rate-limiting enzyme of biosynthesis of polyamines during immune stimuli. Indeed, systemic lipopolysaccharide (LPS) administration increased ornithine decarboxylase (ODC) mRNA and protein within neurons and microglia across the mouse central nervous system (CNS). This treatment was also associated with a robust and transient transcriptional activation of genes encoding pro-inflammatory cytokines and toll-like receptor 2 (TLR2) in microglial cells. The endotoxin increased the cerebral activity of ODC, which was abolished by a suicide inhibitor of ODC. The decrease in putrescine levels largely prevented the ability of LPS to trigger tumor necrosis factor α and TLR2 gene transcription in the mouse brain. In contrast, expression of both transcripts was clearly exacerbated in response to intracerebral spermine infusion. Finally, inhibition of polyamine synthesis abolished neurodegeneration and increased the survival rate of mice exposed to a model of severe innate immune reaction in the CNS. Thus, polyamines have a major impact on the neuronal integrity and cerebral homeostasis during immune insults.

Introduction

Polyamines, namely putrescine, spermidine, and spermine, are essential polycations involved in growth and differentiation (Fozard et al., 1980; Tabor and Tabor, 1984; Pegg et al., 1988). Because high intracellular polyamine levels are known to be detrimental to cells (Auvinen et al., 1992), polyamine content needs to be narrowly regulated by biosynthesis, degradation, and transport systems. Ornithine decarboxylase (ODC;* enzyme classification no. 4.1.1.17) is the first and rate-limiting enzyme in the synthesis of endogenous polyamines. This enzyme catalyzes the conversion of ornithine into putrescine, which is the precursor for higher polyamines. The amount of ODC is regulated by various growth factors and by polyamines at the levels of transcription (Katz and Kahana, 1987), translation (White et al., 1987), and degradation (van Daalen Wetters et al., 1989; Murakami et al., 1992; Matsufuji et al., 1995). Treatment of mammalian tissues with D,L-α-difluoromethylornithine (DFMO), an active-site inhibitor of ODC (Bey et al., 1978; Meyskens and Gerner, 1999), leads to a decrease in intracellular polyamine contents (Hillary and Pegg, 2003). Spermidine and spermine originate from the successive transfers of aminopropyl moiety of decarboxylated S-adenosylmethionine to the secondary amines of putrescine. Spermine and spermidine can be retroconverted in spermidine and putrescine, respectively, by the polyamine interconversion pathway, leading to the production of oxidative intermediate products such as 3-aminopropanal.

Polyamines are not only involved in growth and differentiation. In the brain, they modulate the gating of N-methyl-D-aspartate (NMDA) receptors and ion channels (Ficker et al., 1994; Lopatin et al., 1994; Fakler et al., 1995; Williams, 1997) and are involved in neurodegenerative processes (Morrison et al., 1998). Moreover, polyamines have recently been found to alter the inflammatory response in vitro. The

endotoxin lipopolysaccharide (LPS) is able to increase ODC mRNA expression in monocytes (Messina et al., 1990), and spermine inhibits expression of the inducible isoform of nitric oxide synthase in LPS-treated J774.2 macrophages (Szabo et al., 1994). Intracellular polyamine levels were also found to alter macrophage-mediated cytotoxicity in vitro (Tjandrawinata et al., 1994). Furthermore, the release of pro-inflammatory cytokines by monocytes is inhibited by spermine in a spermine uptake–dependent mechanism (Zhang et al., 1999). Spermine can also increase IL-10 synthesis and suppress IL-12p40 and IFN-γ production in LPS-stimulated macrophages (Hasko et al., 2000).

Spermine is produced at high levels in regenerating tissues and is released into the extracellular medium during cellular lysis (Clarke and Tyms, 1991). Such high levels of polyamines have previously been reported to be toxic for the brain, especially when oxidative products are generated by the interconversion pathway (for review see Seiler, 2000). Independently of the toxicity of its metabolites though, spermine can inhibit in a dose-dependent manner the release of tumor necrosis factor α (TNF-α) in LPS-treated human monocytes (Zhang et al., 1997). These data indicate that at least in vitro, spermine has anti-inflammatory properties (for review see Zhang et al., 2000).

The innate immune system is characterized by an unspecific and rapid response to microbial components as various as peptidoglycan, lipoproteins, lipoteichoic acid, bacterial CpG DNA, and also the endotoxin LPS. This latter is a major glycolipid constituting the outer membrane of gram-negative bacteria. LPS is well known to activate macrophages and trigger the release of pro-inflammatory cytokines as well as arachidonic acid metabolites, and therefore is widely used as a model to trigger the innate immune system (Taveira da Silva et al., 1993). Acute endotoxemia provokes a sharp and transient induction of pro-inflammatory signaling events and transcription of genes that encode cytokines, chemokines, enzymes, proteins of the complement system, and toll-like receptor 2 (TLR2) in the central nervous system (CNS; for review see Nguyen et al., 2002). Therefore, the goal of the work was to determine whether polyamines have the ability to modulate the inflammatory reaction taking place in the brain. The data that a single systemic bolus of LPS caused a robust increase in ODC mRNA expression in numerous structures across the brain suggested a potential role of polyamines in the cascade of neuroinflammatory events. Then, we used different approaches and markers to ascertain the critical role of polyamines in the cerebral innate immunity in vivo. Furthermore, the functional role of polyamines in a model of neurodegeneration was investigated. Altogether, these data support a critical role of polyamines in the control of innate immune response in the brain, which has profound consequences on the neuronal integrity.

Results

Expression of ODC mRNA and protein in the CNS of vehicle- and LPS-treated mice

The distribution of ODC mRNA in vehicle-treated animals is in accordance with a previous report from Kilpelainen et al. (2000). Fig. 1 depicts representative examples of the pattern of ODC gene expression in the mouse brain. Constitutive mRNA levels were found in the cortex (layers c2 to c6), ependymal cells lining the walls of lateral ventricles (epd),
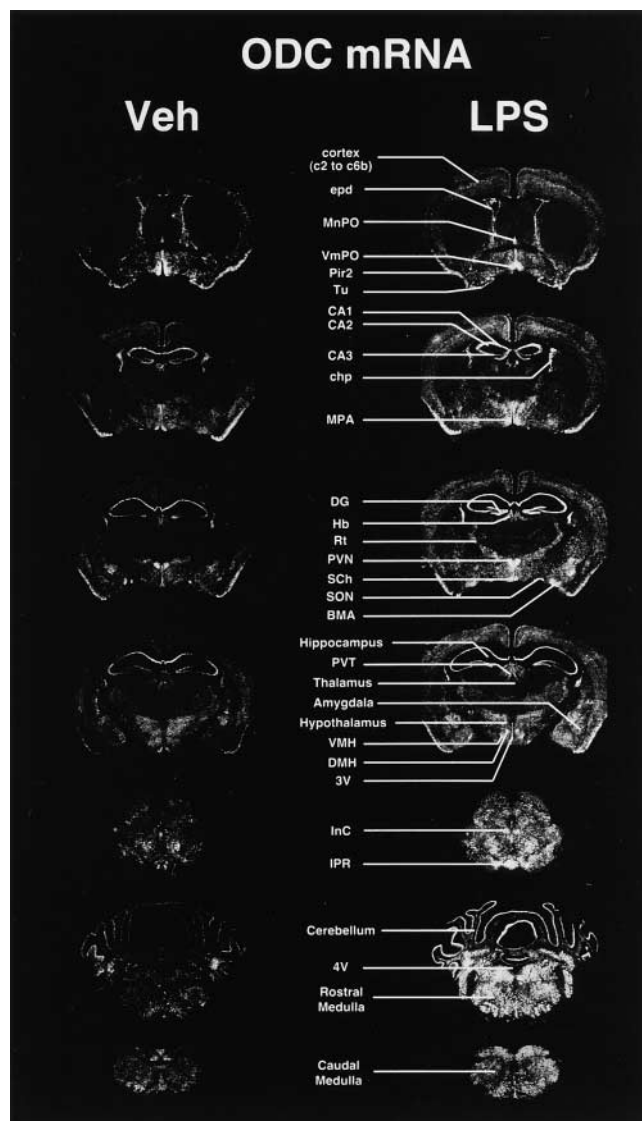

Figure 1. **Expression of the gene encoding ODC in the mouse brain under basal and immune-challenged conditions.** These darkfield photomicrographs of nuclear emulsion–dipped sections represent the hybridization signal of ODC mRNA 24 h after a single systemic bolus of lipopolysaccharide (LPS, 1 mg/kg body weight) or the vehicle solution (Veh). Please note the widespread distribution of ODC transcript across the CNS and the robust increase in the expression levels after systemic LPS administration (right column). 3V, third ventricle; 4V, fourth ventricle; BMA, basomedial nucleus of the amygdala; CA1–3, hippocampal areas; chp, choroid plexus; CPu, caudate putamen; DG, dentate gyrus; DMH, dorsomedial nucleus hypothalamus; epd, ependymal lining cells of ventricle walls; Hb, habenula; InC, interstitial nucleus of Cajal; IPR, interpeduncular nucleus rostral; MnPO, median preoptic nucleus; MPA, medial preoptic area; Pir2, pyriform cortex (pyramidal layer); PVT, paraventricular nucleus of the thalamus; PVN, paraventricular nucleus of the hypothalamus; SCh, suprachiasmatic nucleus: SON, supraoptic nucleus; Rt, reticular nucleus; Tu, olfactory tubercle; VmPO, ventromedial preoptic nucleus; VMH, ventromedial nucleus hypothalamus. Magnification, 1.65.
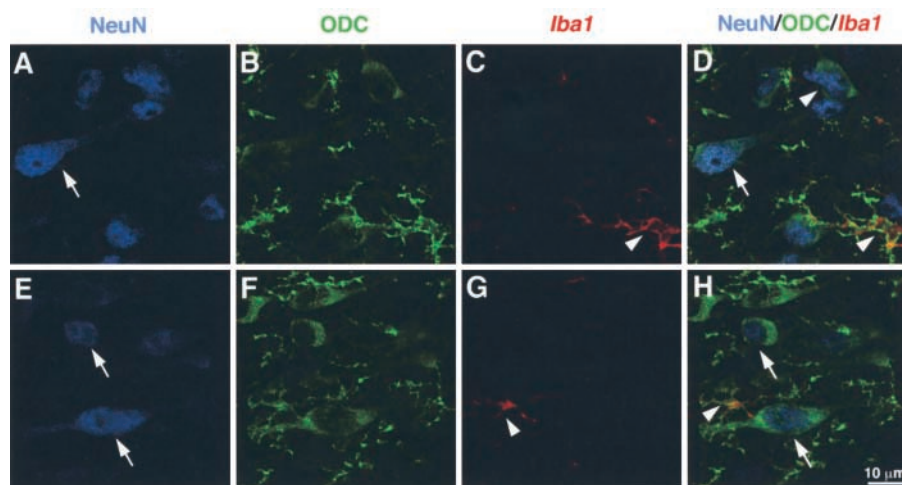
Figure 2. **Confocal laser scanning microscopic image of ODC-immuno-reactive (ir) signal within neurons and microglia in the cerebral cortex.** Neuronal nuclei were labeled by means of a primary antibody directed against NeuN and a secondary antibody conjugated to Alexa Fluor® 546 (A and E, blue nuclei). The secondary antibody used to label ODC was coupled to Cy2 (B and F, green), whereas a Cy5 secondary antibody was used to bind the primary antibody directed against ionized calcium binding adaptor molecule 1 (C and G, *iba1*) expressed within cells of myeloid lineage (red). D is an overlay of A–C. H is an overlay of E–G. White arrows show double-labeled neurons (ODC-ir/NeuN-ir), whereas white arrowheads show double-labeled microglial cells (ODC-ir/*iba1*-ir).

median preoptic nucleus (MnPO), ventromedial preoptic nucleus (VmPO), medial preoptic area (MPA), piriform cortex 2 (Pir2), and olfactory tubercle (Tu). Hippocampal CA1, CA2, CA3, and dentate gyrus (DG) exhibited strong constitutive mRNA levels, but the signal was barely detectable in the basal ganglia and thalamic area. In the latter, the hybridization signal was positive only in the habenula (Hb), paraventricular thalamic nucleus (PVT), and reticular nucleus (Rt). On the other hand, numerous nuclei and areas of the hypothalamus and amygdala contained basal ODC mRNA levels. The intensity of the message was actually quite robust in the paraventricular nucleus (PVN), suprachiasmatic nucleus (SCh), dorsomedial hypothalamus (DMH), ventromedial hypothalamus (VMH), and supraoptic nucleus (SON). The transcript was also detected in the choroid plexus (chp), purkinje cell layer of the cerebellar cortex, and numerous nuclei and regions of the rostral and caudal medulla (Fig. 1, bottom left).

The hybridization signal was clearly more intense in the brain of mice that received a single systemic bolus of LPS (Fig. 1, right column). The increase in ODC mRNA levels was nevertheless not specific and took place in most of the constitutively expressing regions, although differences were noted among animals, nuclei, and regions. The medulla was particularly sensitive to the treatment and exhibited very strong expression levels, especially at 24 h after LPS administration (Fig. 1, bottom right).

To ascertain the cellular localization of ODC in the untreated mouse brain, a multiple labeling approach was performed. As depicted by Fig. 2, the positive signal in both neuronal and microglial cells was confirmed via triple immunohistochemistry labeling and confocal laser scanning microscopy. Cytoplasmic ODC protein (Fig. 2, green) colocalized with the specific marker of neuronal nuclei NeuN (Fig. 2, blue), which provides the anatomical evidence that neurons have the ability to produce polyamines. ODC-immunoreactive cells also colocalized with a marker of microglial cells, *iba1*. (Fig. 2, red). However, ODC⁺/NeuN⁺ cells were clearly more numerous and widely distributed than ODC⁺/*iba1*⁺ cells across the cerebral tissue of mice injected systemically with the bacterial cell wall component.

ODC activity in the CNS of vehicle- and LPS-treated mice

The ODC protein is a particular enzyme well known for its extremely short half-life and its narrowly controlled transcription, translation, and activity. To ensure that LPS-induced increase in ODC gene expression was really associated with putrescine biosynthesis, ODC activity was measured in one hemisphere of each control and treated mouse (Fig. 3). In accordance with other reports, a low level of ODC activity was found in the brain of control mice (Kilpelainen et al., 2001). Cerebral ODC activity was not significantly different between control mice and those that were treated with DFMO. However, ODC activity was strongly induced by sixfold 3 h after a single systemic injection of LPS, which indicates that the latter is able to increase the biosynthesis of putrescine in the brain. The enzymatic activity was reduced by 50% in mice that had access to DFMO in their tap water for 2 d before the systemic LPS challenge. These data demonstrate the ability of DFMO to cross the blood-brain barrier (BBB) and inhibit the ODC protein within the brain.
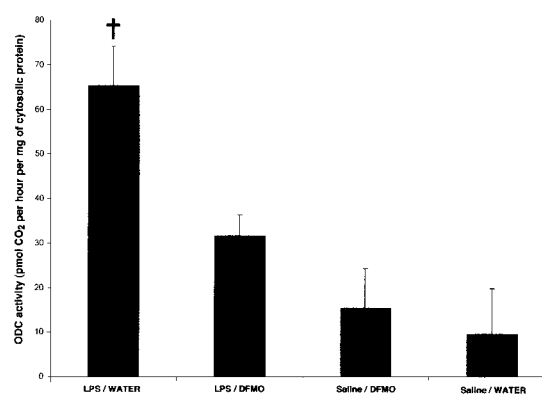

Figure 3. **Effects of LPS and DFMO treatments in the brain ODC activity.** ODC activity was determined as described in Materials and methods. Data are mean ± SEM (bars) values of four animals. †, significantly different (P < 0.005) from all the other groups of mice.
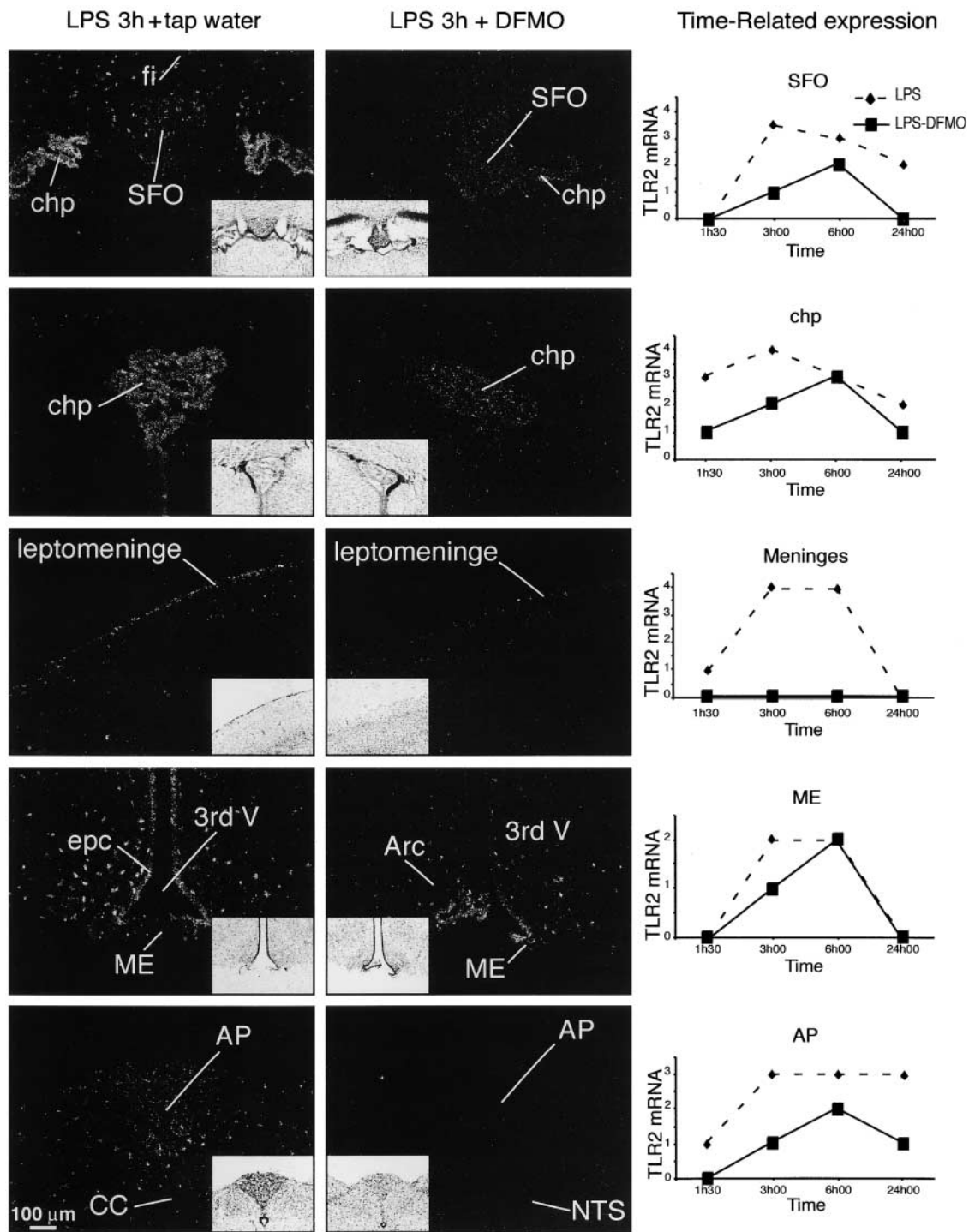
Figure 4. **Effects of DFMO on the transcriptional activation of TLR2 in the brain of mice challenged systemically with the endotoxin LPS.** These photomicrographs were taken from mice that had free access to tap water or the suicide inhibitor of ODC DFMO (2% in drinking water) for a period of 2 d before the single i.p. LPS bolus. The brightfield images (insets) are the corresponding darkfield photomicrographs of nuclear emulsion–dipped sections of mice killed 3 h after the LPS challenge. The plotting graphs of the right column depict the time-related induction of the gene encoding TLR2 in each corresponding area, namely subfornical organs (SFO), choroid plexus (chp), leptomeninges, median eminence (ME), and area postrema (AP). Please see Materials and methods for the qualitative analysis of the hybridization signal. 3rd V, third ventricle; CC, central canal; epc, ependymal cells; fi, fimbria of hippocampus; NTS, nucleus of the solitary tract. Hyphenated lines (◆) represent the tap water/LPS group, whereas solid lines (■) show the data for the DFMO/LPS group of mice.

Time-related inhibition of TLR2 mRNA by DFMO

TLR2 mRNA has previously been reported to be a very sensitive inducible transcript involved in the early innate immune response to microbial challenge, and was therefore used in this present work as a marker of neuroinflammation. A single i.p. bolus of LPS caused a strong transcriptional activation of TLR2, first within structures devoid of BBB, and thereafter across deeper parenchymal areas of the brain. In-

deed, the hybridization signal was rapidly detected in cells lining the leptomeninges, chp, all the circumventricular organs (CVOs), and along few blood vessels (Fig. 4). Parenchymal cells in the regions adjacent to these structures became gradually positive, and the signal spread across the cerebral tissue 24 h after LPS injection. Previously, we have reported that such a migratory-like induction pattern takes place essentially within macrophages/microglial cells (Laflamme et al., 2001). Putrescine plays a critical role in this innate immune response because TLR2 expression levels were much lower across the cerebral tissue of animals that had free access to DFMO (2% drinking water) for a period of 2 d before the systemic LPS challenge. Indeed, TLR2 hybridization signal was higher in all the regions analyzed in the brain of mice that had tap water instead of DFMO (Fig. 4). Inhibition of ODC by DFMO largely abolished the spreading of TLR2-expressing cells across the cerebral tissue, and leptomeninges no longer displayed positive signal in mice treated with LPS and DFMO at all the times evaluated in this work. This treatment was also able to significantly prevent LPS-induced transcriptional activation of the proinflammatory cytokine TNF-α in regions devoid of BBB as well as in the brain parenchyma (unpublished data). These data clearly support the involvement of polyamines in the control of the innate immune response by microglial cells.

Induction of TLR2 and TNF-α transcripts by intracerebroventricular injection of spermine

The next series of experiments tested the effects of spermine on the innate immune response in the CNS. In contrast to DFMO, intracerebroventricular (i.c.v.) spermine administration exacerbated the effects of LPS on TLR2 and TNF-α gene expression in the mouse brain (Fig. 5). Animals that received the intracerebral spermine treatment before the systemic LPS injection exhibited a profound transcriptional activation of TLR2 in the chp, CVOs, leptomeninges, microcapillaries, and within small, scattered cells across the cerebral tissue (Fig. 5, second left column). This was also the case for the proinflammatory cytokine TNF-α, especially within small, scattered cells in the brain parenchyma. Indeed, TNF-α–expressing cells were clearly more numerous and widely spread throughout the CNS of mice that were killed 6 h after being injected with spermine before the endotoxin (right column). TLR2 and TNF-α mRNA levels increased by 560 and 35%, respectively, in response to spermine/LPS treatment when compared with the signal intensity quantified in the cerebral tissue of mice challenged only with the bacterial endotoxin (Fig. 5, bottom). Nevertheless, the polyamine is not by itself an immune stimulus for microglial cells because the treatment with spermine alone failed to trigger TLR2 and TNF-α gene expression in the mouse CNS (Fig. 5, bottom).

Effects of DFMO on the ability of LPS to cross the BBB

LPS uptake in brain parenchyma was monitored by immunohistochemistry using an antibody directed against lipid A, which is the conserved part of the endotoxin. Lipid A immunoreactivity remained undetectable in brain parenchyma of mice that received either vehicle or LPS (Fig. 6, A and C). This phenomenon was also similar in the CNS of mice that

were pretreated with DFMO (Fig. 6 D), which indicates that DFMO did not increase or change the permeability of the BBB to the endotoxin, at least when injected systemically and as measured by lipid A immunoreactivity. On the other hand, a very strong immunoreactive signal was detected in the brain of mice that has a single bolus of LPS into the striatal region (Fig. 6 E). These data provide the evidence that the anti-lipid A antibody was capable of recognizing the endotoxin within the brain parenchyma.

Functional role of polyamines in a model of inflammation-induced neurodegeneration

To determine whether the ability of polyamines to alter the inflammatory response may be associated with functional consequences on the neuronal integrity, mice received a single systemic injection with the glucocorticoid (GC) receptor inhibitor RU486 before an intracerebral bolus of LPS. This treatment is known to cause an exaggerated inflammatory reaction due to the lack of inhibitory feedback of GCs on microglial cells, which ultimately leads to neurodegeneration (Nadeau and Rivest, 2003). Anatomical signs of brain damages were detected 3 d after the dual treatment combining intracerebral LPS and systemic RU486 (Fig. 7, A and B). Infusion of the endotoxin alone directly into the brain parenchyma failed to provoke neurodegeneration despite the robust and transient innate immune reaction (Nadeau and Rivest, 2002; unpublished data). Indeed, brain damages took place only in mice that received RU486 before the intracerebral LPS insult (Fig. 7 A, white area into the dotted-line circle). The fluorochrome Fluoro-Jade B (FJB) was also used to determine the extent of the neurodegenerating area, which can be visualized by the FJB green staining (Fig. 7 B). Pretreatment with DFMO essentially abolished the effects of the combined injections of RU486 and LPS (Fig. 7, C and D). Indeed, the brain of mice that had free access to DFMO for a period of 2 d before LPS and RU486 insults did not exhibit any signs of neurodegeneration except for the tract made by the infusion cannula.

In addition to its neuroprotective role, DFMO was able to increase dramatically the survival rate of mice treated with RU486/LPS (Fig. 7 E). 66% of the mice survived to this treatment when they were pretreated with DFMO for 2 d before surgery (yellow line), whereas most (93%) mice that did not have access to DFMO died within 2 h in response to the RU486/LPS treatment (red line). Actually, only one mouse survived in that group and was used for the histological preparations depicted in Fig. 7, A and B. Inhibition of putrescine synthesis was able to prevent the neurotoxic effects of an intracerebral LPS infusion in the absence of an appropriate negative feedback of GCs on the innate immune response in the CNS. These data provide the first in vivo evidence that polyamines are essential modulators of the cascade of neuroinflammatory events, which may ultimately have profound impacts on the neuronal elements and the survival of the host during intracerebral infections by gram-negative bacteria.

Discussion

This is the first paper investigating the role of polyamines in the brain in vivo in a neuroinflammatory context. Here, we
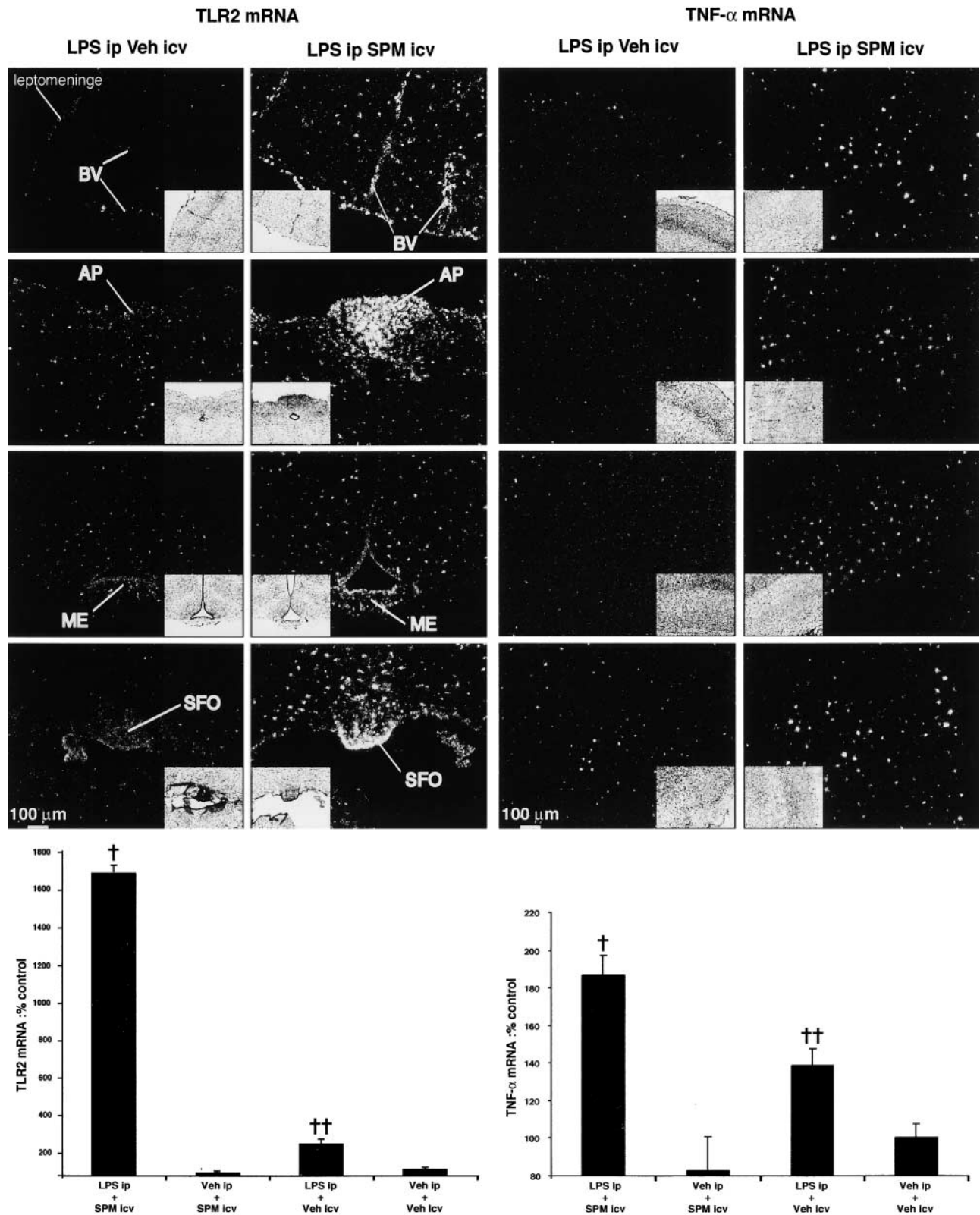
Figure 5. **Exacerbation of the innate immune response by i.c.v. spermine administration.** Mice received a 100-nmol i.c.v. bolus of spermine or vehicle solution 5 min before the i.p. LPS challenge, and were killed 6 h after injection time. The brightfield images (insets) are the corresponding darkfield photomicrographs of nuclear emulsion–dipped sections hybridized with either toll-like receptor 2 (TLR2) or tumor necrosis factor α (TNF-α) cRNA probe. Please note the robust and widespread hybridization signal for both transcripts in the brain of mice that received both i.c.v. spermine and i.p. LPS. The plotting graphs depict the semi-quantitative analysis of hybridization signal performed as described in Materials and methods. Data are means (± SEM) percentage of the control group (vehicle i.c.v/vehicle i.p.). BV, blood vessels; AP, area postrema; ME, median eminence; SFO, subfornical organ. †, significantly different ($P < 0.05$) from the other groups. ††, significantly different ($P < 0.05$) from both groups of vehicle-treated mice.
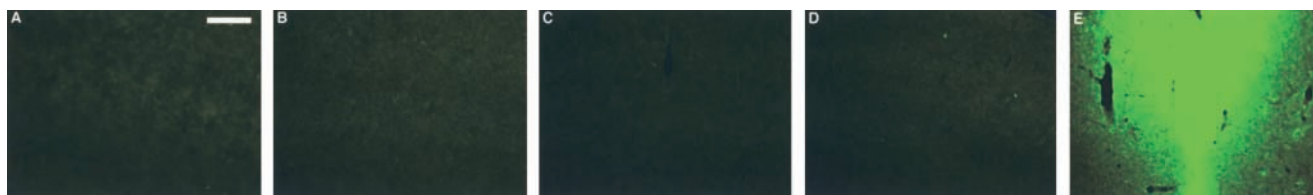
Figure 6.   **Inhibition of ODC does not alter the entry of LPS in brain parenchyma.** Animals had free access to tap water (A, C, and E) or DFMO (2% in drinking water, B and D) for a period of 2 d before the systemic LPS (C and D) or saline (A and B) injection. The endotoxin was also injected directly within the mouse dorsal basal ganglia as positive control (E). Brains were collected 3 h after the injections and processed for immunohistochemistry. Anti-lipid A antibody was used as marker for the conserved part of LPS (green). Please note the strong immunoreactive signal only in the brain of the mouse that was administered with the endotoxin directly into the cerebral tissue, whereas no signal was found in the parenchymal brain of mice that had access or not to DFMO in their tap water and challenged with LPS i.p. Exposure time, 9 s. Bar, 50 μm.

show that polyamines are involved in the control of the innate immune system in the CNS and may have a determinant impact on the inflammatory events that take place during bacterial infection. Indeed, a single systemic injection with a cell wall component derived from gram-negative bacteria caused robust increase in the gene encoding the first and rate-limiting enzyme of endogenous synthesis of polyamines. The increase in ODC mRNA expression is in agreement with a previous paper that found up-regulation of ODC transcription in monocytic cells exposed to LPS (Zheng et al., 1991). We use this model of systemic endotoxemia because it has the ability to increase the innate immune response in the brain, which is associated with transcriptional activation of numerous pro-inflammatory genes in microglial cells (Nadeau and Rivest, 2000, 2001; Laflamme and Rivest, 2001; Laflamme et al., 2001; Nguyen et al., 2002).

ODC is narrowly regulated at the level of transcription, translation, and post-translation (Katz and Kahana, 1987; White et al., 1987; van Daalen Wetters et al., 1989; Matsufuji et al., 1995). Therefore, changes in mRNA levels may not reflect increase in ODC activity and polyamine biosynthesis in the cerebral tissue of LPS-treated mice. The presence of antizyme (Kilpelainen et al., 2000), the inhibitor of ODC, could also restrain the biosynthesis of polyamines in the brain. However, ODC activity was strongly induced in the brain of LPS-injected mice, which provides compelling evidence that this immune challenge is not only capable of triggering ODC transcription, but also putrescine biosynthesis within the cerebral tissue. Moreover, the ability of DFMO to alter both ODC activity and innate immune response to LPS indicates that polyamine biosynthesis is indeed taking place in the cerebral environment. The fact that intracerebral spermine infusion was able to exacerbate the effects of LPS adds further evidence that spermine, the most downstream polyamine from putrescine, is involved in the control of the inflammatory response in the CNS. It is interesting to note that the effects of DFMO on brain ODC activity were found only in LPS-challenged mice. Basal ODC activity is usually extremely low in the adult mouse CNS (2.83 ± 0.71 pmol CO_2 per h and per mg protein; Kilpelainen et al., 2001), and ODC assay was performed with a protocol designed originally for ODC activity in the prostate, the tissue that exhibits the highest ODC activity under basal conditions (Kilpelainen et al., 2001). In the present method, ODC activity was close to the limit of quantification in the brain of control mice, but DFMO had clear effects on the enzyme activity in LPS-challenged ani-

mals. This is nonetheless not surprising because DFMO has been widely used as an ODC inhibitor, which usually leads to a complete depletion of putrescine contents as well as a significant decrease in spermidine and spermine levels (Gilad and Gilad, 2002; Hillary and Pegg, 2003).

Then, we verified whether microglial cells that are the resident macrophages of the brain were also capable of expressing ODC in response to the endotoxin. This was confirmed by multiple labeling and confocal microscopy approaches, and it is clear from these data that circulating LPS increases ODC gene expression within neurons and microglial cells. These data provide anatomical evidence that although regulation of gene encoding ODC takes place within neurons and microglia, pro-inflammatory transcripts are up-regulated essentially within microglia. These cells play a critical role in the control of the innate immune response, and are under the control of polyamines because the suicide inhibitor of ODC DFMO significantly prevented the increase in TLR2 and cytokine mRNA levels in response to circulating LPS. Although TLR2 is the receptor that recognizes gram-positive bacteria, its promoter is very sensitive to ligands that trigger nuclear factor kappa B signaling, and LPS has the ability to increase TLR2 transcription first within structures devoid of BBB and thereafter in microglial cells across the brain parenchyma (Laflamme et al., 2001; Nguyen et al., 2002). The fact that DFMO dramatically inhibited the effects of LPS on TLR2 and cytokine gene expression in all these regions indicates that decrease in putrescine levels is a profound endogenous anti-inflammatory mechanism in the brain.

The present data supporting that polyamines act as proinflammatory molecules are in disagreement with in vitro reports in which spermine was found to inhibit cytokine synthesis in macrophages in culture (Zhang et al., 1997, 1999, 2000). However, this discrepancy can be explain by the fact that the present experiments were performed in an in vivo model in the brain where microglial cells, the CNS resident macrophages, are in narrow paracrine relationships with other cells, such as astrocytes and neurons. Another major difference is that unlike in vivo, LPS may not be eliminated in culture, and chronic exposure to the endotoxin is known to cause tolerance of immune cells to this ligand (Nomura et al., 2000). Tolerant macrophages may behave quite differently to polyamines from parenchymal microglia that were activated in an acute manner in the present work.

The mechanism mediating the effects of circulating LPS on ODC induction across the cerebral elements remains un-
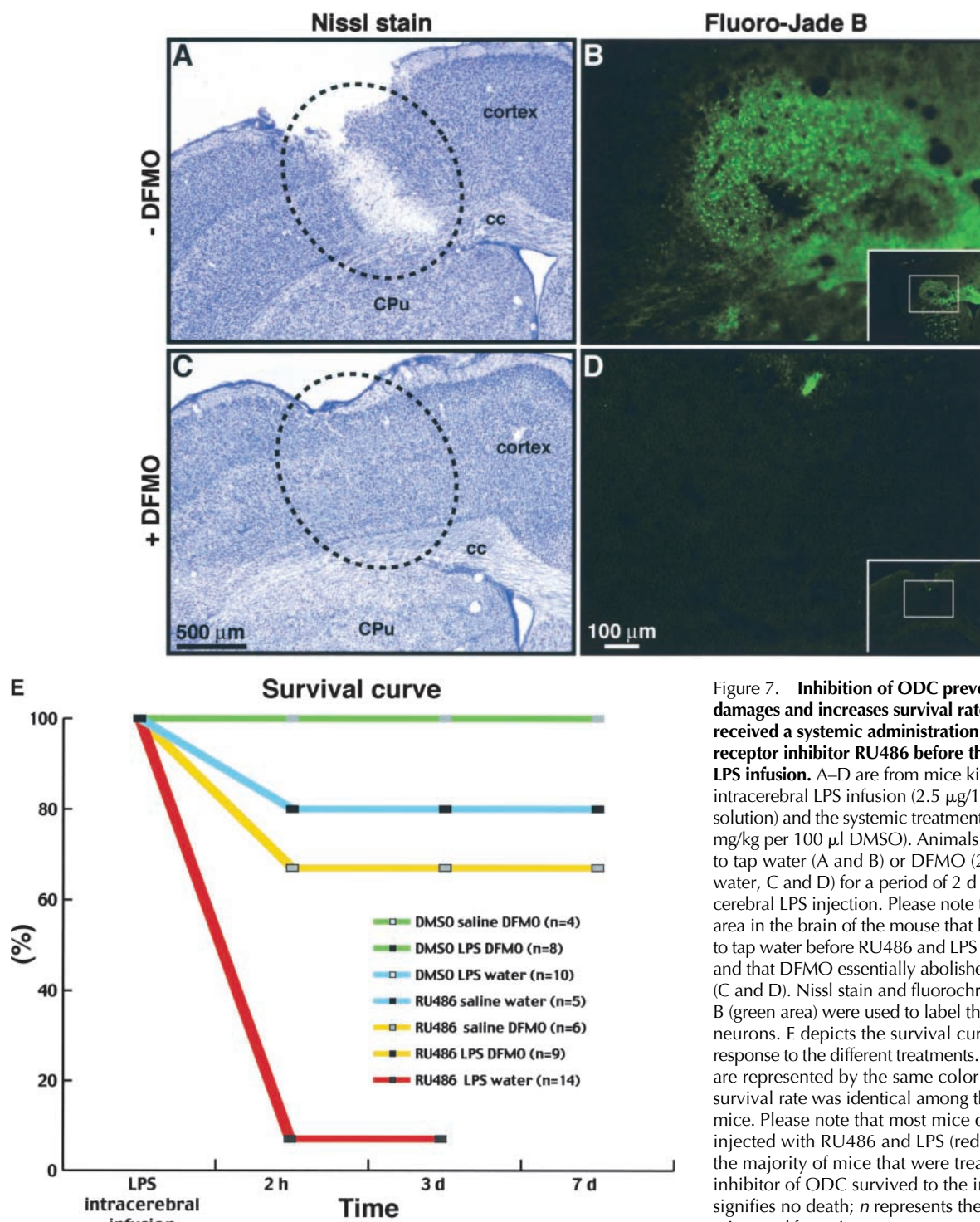
Figure 7.   **Inhibition of ODC prevents cerebral damages and increases survival rate of mice that received a systemic administration with the GC receptor inhibitor RU486 before the intracerebral LPS infusion.** A–D are from mice killed 3 d after the intracerebral LPS infusion (2.5 μg/1 μl sterile saline solution) and the systemic treatment with RU486 (50 mg/kg per 100 μl DMSO). Animals had free access to tap water (A and B) or DFMO (2% in drinking water, C and D) for a period of 2 d before the intracerebral LPS injection. Please note the degenerating area in the brain of the mouse that had only access to tap water before RU486 and LPS insults (A and B), and that DFMO essentially abolished these effects (C and D). Nissl stain and fluorochrome Fluoro-Jade B (green area) were used to label the degenerating neurons. E depicts the survival curve of mice in response to the different treatments. Some treatments are represented by the same color because the survival rate was identical among these groups of mice. Please note that most mice died after being injected with RU486 and LPS (red line), whereas the majority of mice that were treated with the inhibitor of ODC survived to the insults. 100% signifies no death; *n* represents the total number of mice used for a given treatment. cc, corpus callosum; CPu, caudate putamen.

clear at this point. Immunohistochemistry was performed to label lipid A, which is the conserved part of LPS. The latter was not detectable in the parenchymal brain of mice that received a single i.p. bolus of LPS, and DFMO did not affect the entry of LPS across the BBB. Therefore, it seems that LPS is not directly responsible to trigger ODC activity in parenchymal elements of the brain, but this phenomenon may be attributable to intermediate factors. Indeed, production of TNF-α by cells of the chp and CVOs may be a deter-

minant endogenous mechanism involved in this process. Microglial TNF-α acts as an autocrine and paracrine factor to trigger the inflammatory reaction in the CNS during endotoxemia (Nadeau and Rivest, 2000; Nguyen et al., 2002), and this elegant mechanism is likely to explain the effects of circulating LPS on ODC in the CNS. However, we have yet to provide direct evidence supporting this cascade of events.

This issue regarding whether circulating LPS and other pathogen-associated molecular patterns have the ability to

reach parenchymal elements of the brain still remains a matter of controversies. Injection with the bacterial endotoxin has been shown to cause a 36% increase in ion permeability of the BBB (Dyatlov et al., 1998) and elicit gaps between brain microvasculature endothelial cells with bulging of nuclear zones and increased numbers of vesicular Golgi complexes and ER (Persidsky et al., 1997). Lustig and colleagues have also reported that LPS can contribute to virus penetration from the blood into the CNS, a process that turns a mild viral infection into a severe lethal encephalitis caused by injury to cerebral microvasculature endothelium and modulation of BBB permeability (Lustig et al., 1992). In contrast, an opening of the BBB was observed during cerebral inflammatory responses (allergic encephalomyelitis), but not after LPS administration (de Vries et al., 1995). Despite the fact that LPS decreases endothelial resistance that may lead to enhanced transport of low and high mol wt molecules, whether the endotoxin can easily diffuse through the BBB and whether it can reach deep parenchymal brain are still open questions, and such a mechanism was not supported by the present paper.

Polyamines have the ability to modulate the immune response only in the presence of LPS, and spermine alone is unable of mimicking the effects of the endotoxin. Therefore, polyamines are not direct ligands for activating pro-inflammatory signaling and gene expression by microglial cells, at least

in the present model. The brains of animals that received DFMO or spermine alone were comparable to those of vehicle-treated mice. However, polyamines seem required to transduce the secondary signal-taking place across microglial cells of LPS-treated mice. How then, do polyamines modulate the innate immune response in the CNS? They may directly alter LPS-induced signal transduction and gene expression in microglial cells (Fig. 8, model 1). Alternatively, spermine originating from neurons and microglia could exert toxic effects either by the formation of oxidative products along the interconversion pathway (Fig. 8, model 2 A) and/or by an excitotoxic processes via overactivation of NMDA receptors (Fig. 8, model 2 B). Both cases would lead to an early innate immune reaction and gene expression by microglial cells. Another possibility would be the ability of extracellular spermine to act directly on microglial cells via the polyamine transport system (Fig. 8, model 2 C) and to modulate the transcription of early genes involved in the control of the innate immune system.

The physiological relevance of such interaction between polyamines and the innate immune system in the brain has yet to be clearly established. Increase in polyamine metabolism was found to be neurotoxic via glutamate-induced excitotoxic events and oxidative by-products originating from the polyamine interconversion pathway (Porcella et al., 1991). In contrast, this pathway may play a critical role in
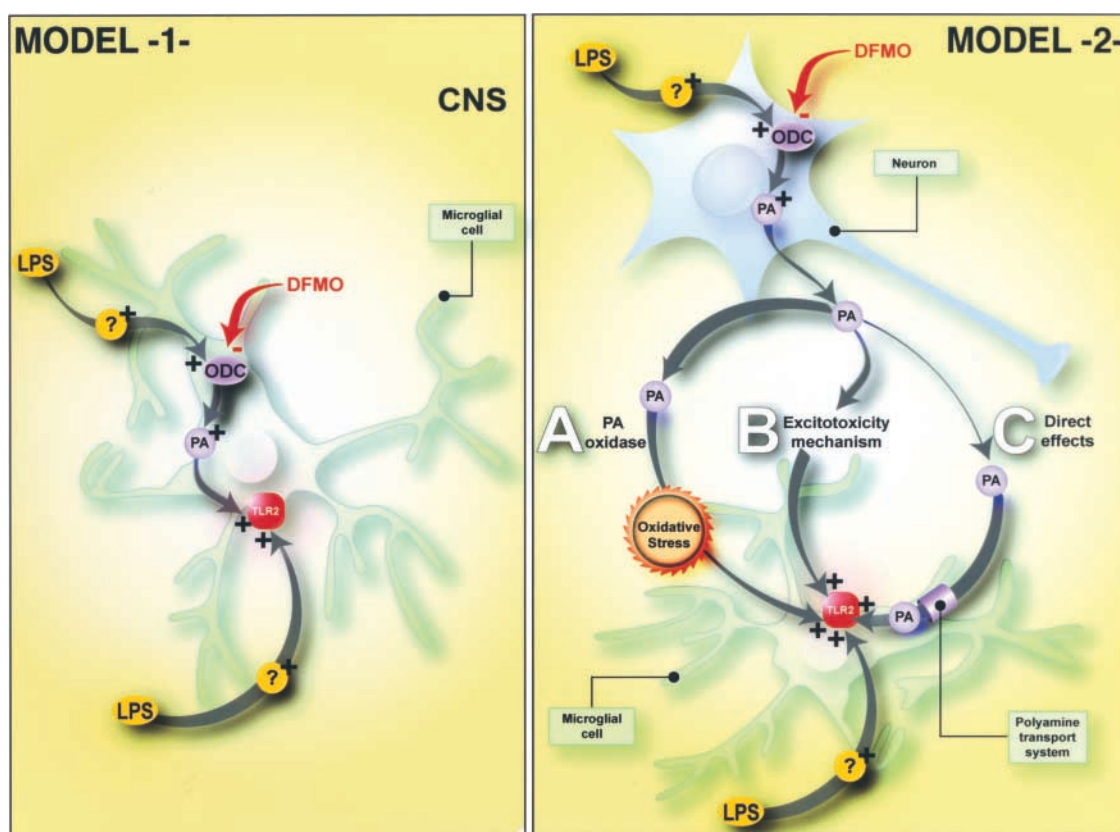

Figure 8.   **Illustration depicting various hypothetical pathways by which polyamines may interact directly or indirectly with microglial cells to modulate the innate/inflammatory response in the CNS.** Model 1, LPS induces ODC expression in microglial cells, which leads to an increase of intracellular polyamine (PA) concentrations to a level required for TLR2 induction. Model 2, LPS induces neuronal ODC expression and increases PA levels. DFMO inhibits ODC activity, which leads to a decrease in putrescine levels. PAs are released in the extracellular compartment and exacerbate LPS-induced TLR2 transcription in microglia by three potential pathways. (A) Interconversion of PAs and generation of oxidative by-products. (B) Excitotoxicity mediated via PA-activated NMDA receptors. (C) Direct interaction in microglial cells subsequent to PA internalization via PA transport systems. Please see Discussion for details.

neuronal survival after cerebral ischemia (Gilad and Gilad, 1988). Spermine is also able to act as a free radical scavenger (Ha et al., 1998), which could be a neuroprotective mechanism in the presence of free radicals in the cerebral environment. It is also possible that ODC contributes to the growth and plasticity of specific groups of neurons because polyamines are involved in the development of the CNS (Shimizu et al., 1965) and of axonal regeneration after injury (Cai et al., 2002). Nevertheless, it remains unclear why ODC expression levels are high in some groups of neurons and undetectable in others, such as the basal ganglia.

To understand the functional role of polyamines in the CNS as being neurotoxic and/or neuroprotective molecules, we used a model of neurodegeneration caused by an exaggerated inflammatory response. GCs are probably the most powerful endogenous immunosuppressors, especially for the innate immune response and the subsequent inflammatory reaction (McKay and Cidlowski, 1999). Indeed, GCs are potent inhibitors of transcription of genes encoding most of the proteins involved in the innate immune system, and a large body of evidence suggests that nuclear factor kappa B is a key step in this process (McKay and Cidlowski, 1999). Altogether, these effects of GCs ultimately lead to a decrease in pro-inflammatory signal transduction pathways and gene expression, which is an essential endogenous mechanism to avoid exaggerated responses during immunogenic challenges. As expected, the inflammatory response lasted longer in the brain of animals that received the GC receptor antagonist RU486 before the intracerebral LPS infusion (Nadeau and Rivest, 2002). Surprisingly, a single bolus of LPS caused a rapid and severe neurodegeneration only in RU486-pretreated animals (Nadeau and Rivest, 2003). This was also the case in the present work because no sign of degeneration was found in the brain of mice challenged intracerebrally with LPS and vehicle i.p., but the endotoxin became highly neurotoxic in mice treated with RU486. In this model, the stress was so intense that most of mice died within 2 h after LPS infusion; the only surviving mouse exhibited major neuronal damages at the site of LPS administration. The decrease in putrescine levels by DFMO before the RU486/LPS cotreatment was able to increase the survival rate from 7 to 66%, and was able to protect LPS-induced neurodegeneration due to inhibition of GC receptors in the brain. Therefore, polyamines are powerful neurotoxic molecules in this model of exaggerated innate immune reaction.

In conclusion, polyamines play a major role in the control of the cerebral innate immune response during microbial challenges. These data may have a major clinical impact and suggest DFMO as a potential therapeutic drug to restrain neurodegeneration in brain disorders associated with inflammation. The exact mechanisms involved with the cytotoxic effects of polyamines still need to be firmly established, but the ability of DFMO to prevent LPS-induced TNF-α and the critical role of this cytokine in the LPS/RU486 model (Nadeau and Rivest, 2003) lead to this direction for future investigations.

Materials and methods

Animals
136 adult male CD1 mice ($\sim$25–30 g; Charles River Canada) were acclimated to standard laboratory conditions (14 h light/10 h dark cycle, lights on at 06.00 and off at 20.00) and were given free access to chow and wa-

ter. Animal breeding and experiments were conducted according to the Canadian Council on Animal Care guidelines, as administered by the Laval University Animal Care Committee.

Experimental protocols
The first experiment was performed to determine the expression pattern of the gene encoding ODC in the brain of mice under basal and immune-challenged conditions. To this end, mice received a single i.p. bolus of either 1 mg/kg LPS (from *Escherichia coli,* serotype 055:B5, lot 58H4076; Sigma-Aldrich) or vehicle solution (100 µl sterile, pyrogen-free saline), and were killed 1.5, 3, 6, and 24 h afterward as explained below. A second group of animals was pretreated with the suicide inhibitor of ODC DFMO (Ilex Oncology) for 48 h. The drug was diluted at a concentration of 2% in the drinking water, whereas the control group had access to tap water. 2 d after the beginning of the treatment, both groups were injected with either sterile saline or LPS and killed at numerous times after injection.

The third group of mice was temporarily anesthetized via an i.p. injection of a mixture of ketamine hydrochloride, xylazine, and sterile pyrogen-free saline (1.5:0.5:8.5 vol/vol/vol). The right ventricle was reached stereotaxically using the Paxinos and Franklin Atlas (David Kopf Instruments). With the incisor bar placed 2 mm below the interaural line (horizontal zero), the coordinates from bregma for the injection cannula were 0 mm anteroposterior, 1.1 mm lateral, and 2.4 mm dorsoventral. Thereafter, 100 nmol spermine (lot 126H2615; Sigma-Aldrich) or vehicle solution (pyrogen-free, sterile, distilled water) was injected with a cannula (33G; Plastics One) into the right lateral ventricle in a 1-µl volume over 2 min by means of a microinjection pump (model A-99; Razel Scientific Instruments). 5 min later, mice were injected with either LPS or vehicle and were killed at 6 h after injection time.

The fourth series of experiments consisted of determining the functional role of polyamines in a model neurodegeneration provoked by a robust innate and inflammatory response in the CNS. Mice had free access to tap water or DFMO (2% in drinking water) for a period of 2 d before the surgeries. On the day of the experiment, mice received a single i.p. administration with either the GC receptor antagonist RU486 (50 mg/kg body weight/100 µl DMSO) or vehicle (100 µl DMSO). 1 h later, mice were temporarily anesthetized via an i.p. injection of a mixture of ketamine hydrochloride, xylazine, and sterile pyrogen-free saline (1.5:0.5:8.5 vol/vol/vol). The right striatum was reached stereotaxically using the Paxinos and Franklin Atlas (David Kopf Instruments). With the incisor bar placed 2 mm below the interaural line (horizontal zero), the coordinates from bregma for the infusion cannula (33G; Plastics One) were 0 mm anteroposterior, 2 mm lateral, and 3 mm dorsoventral. Thereafter, 2.5 µg LPS (from *E. coli,* serotype 055:B5, lot 58H4076; Sigma-Aldrich) or vehicle solution (pyrogen-free sterile saline) was infused into the right striatum in a 1-µl volume over 2 min by means of a microinjection pump (model A-99; Razel Scientific Instruments). Animals were killed 3 or 7 d after the intracerebral infusion. Animals were anesthetized with a mixture of ketamine hydrochloride and xylazine (5:1 vol/vol) and were rapidly perfused transcardially with 0.9% saline, followed by 4% PFA in 0.1 M borax buffer (pH 9.5 at 4°C). Brains were removed and processed as described previously (Laflamme et al., 2001).

The fifth experiment was performed to verify whether the suicide inhibitor of ODC DFMO was efficient in the brain. Animals were pretreated with 2% DFMO in the drinking water for 48 h, whereas the control group had free access to tap water. 2 d after the beginning of the treatment, both groups received a single i.p. bolus with either sterile saline or LPS (1 mg/kg) and were killed 3 h later. Animals were anesthetized with a lethal mixture of ketamine hydrochloride and xylazine (5:1 vol/vol) and decapitated for a rapid removal of the brains. Cerebral hemispheres were separated and snap frozen in liquid nitrogen.

Determination of ODC activity
The cerebral hemispheres (230–260 mg) were homogenized into 10 ml ice-cold homogenization buffer (50 mM Tris-HCl, pH 7.3, 50 µM pyridoxal phosphate, 1 mM EDTA, and 2.5 mM DL-dithiothreitol) with a Potter homogenizer. The homogenates were centrifuged at 25,000 g for 60 min at 4°C, and the supernatants were used for the measurement of ODC activity and protein content. ODC activity was assayed by determining the amount of $^{14}CO_2$ released from L-[1-^{14}C]ornithine as described previously (Janne and Williams-Ashman, 1971; Marchetti et al., 1988). Protein contents were determined on the cytosolic fraction by the method of Bradford (1976) using bovine gamma globulin as standard.

In situ hybridization and histological procedures
Plasmids were linearized and sense and antisense riboprobes were synthesized as described in Table I. Hybridization histochemical localization of

Table I. **Plasmids and enzymes used for the synthesis of cRNA probes**

Plasmid	Vector	Insert	Antisense probe	Sense probe	Source
Mouse TLR2	pCR® Blunt II	2.248 kb	EcoRV/SP6	SpeI/T7	PCR amplification[a]
Mouse TNF-α	pBlueScript® SK++	1.3 kb	PstI/T3	BamHI/T7	Dr. D. Radzioch, McGill University, Montreal, Canada
Mouse ODC	pT7-T3	1385 bp	XhoI/T3	SphI/T7	American Type Culture Collection, Manassas, VA

[a]The DNA fragment of 2.278 kb corresponding to the almost-complete coding sequence (2.355 kb) of the reported mouse TLR2 mRNA (nucleotide 307–2661; GenBank/EMBL/DDBJ accession no. AF185284) was amplified by PCR from a cDNA macrophage B10R cell line library using a pair of 23-bp oligonucleotide primers complementary to nucleotides 323–345 (5′-GGCTCTTCTGGATCTTGGTGGCC-3′) and 2579–2601 (5′-GGGCCACTCCAGGTAGGTCTTGG-3′).

the different transcripts was performed on every twelfth section of the whole rostrocaudal extent of each brain using ^{35}S-labeled cRNA probes as described previously (Laflamme et al., 1999). Nissl stain was used as a general index of cellular morphology, and neuronal death was determined via the Fluoro-Jade B method (Nadeau and Rivest, 2003).

Triple immunofluorescence for confocal laser scanning microscopy

Mouse anti-neuronal nuclei (NeuN; CHEMICON International), mouse anti-ionized calcium binding adaptor molecule 1 (iba1; provided by Dr. Yoshinori Imai, National Institute of Neuroscience, Kodaira, Japan), and mouse ODC (MP16–2; Neomarkers) antibodies were used for the multiple immunohistochemical labeling. In brief, slices from untreated animals were washed in sterile DEPC-treated 50 mM potassium phosphate-buffered saline (KPBS) and incubated for 20 h at 4°C with ODC antibody diluted in sterile KPBS plus 0.4% Triton X-100, 1% BSA (fraction V; Sigma-Aldrich), and 0.25% heparin sodium salt USP. Brain slices were then rinsed in sterile KPBS and incubated with a mixture of KPBS plus 0.4% Triton X-100, 1% BSA, 0.25% heparin, and secondary antibody (Cy™2-conjugated AffiniPure goat anti–mouse IgG, H+L, 1:1,500 dilution; Jackson ImmunoResearch Laboratories) for 60 min. After several rinses in sterile KPBS, sections were incubated with NeuN and iba1 antibodies for 20 h at 4°C. Thereafter, slices were rinsed in sterile KPBS and incubated for 60 min with a mixture of KPBS plus 0.4% Triton X-100, 1% BSA, 0.25% heparin, and secondary antibodies (Cy™5-conjugated AffiniPure goat anti–rabbit IgG, H+L, 1:1,500 dilution; Jackson ImmunoResearch Laboratories) and Alexa Fluor® 546–conjugated goat anti–mouse IgG (H+L, 1:1,000 dilution; Molecular Probes, Inc.). Brain slices were finally rinsed several times in sterile KPBS, mounted onto gelatin-coated slides, and coverslipped with a polyvinyl alcohol (Sigma-Aldrich) mounting medium containing 2.5% 1,4-diazabicyclo(2,2,2)-octane (Sigma-Aldrich) in buffered glycerol (Sigma-Aldrich).

Confocal laser scanning microscopy

Confocal laser scanning microscopy studies were performed with an oil immersion objective (X100 Plan-Apo, NA 1.35, X2 numerical zoom) and a microscope (BX-61; Olympus). Cy™2, Alexa Fluor® 546, and Cy™5 were excited sequentially at 488 nm (Ar Ion laser; Melles Griot Laser Group) set at 35% of maximum laser power, 543 nm (HeNe-G Laser; Melles Griot Laser Group) set at 25% of maximum laser power, and 647 nm (HeNe-R Laser, Melles Griot Laser Group) set at 25% of maximum laser power, respectively. Emissions from Cy™2-, Alexa Fluor® 546-, and Cy™5-labeled antibodies were recorded by photomultipliers preset respectively for EGFP (green pseudo color), TRITC (blue pseudo color), and Cy™5 (red pseudo color) fluorescent dyes in Fluoview SV 500 imaging software (Olympus). 13 1-μm confocal z-series were acquired for each area and were corrected by 2 Kahlman low speed scans. Acquired z-series images were then flattened in one image and exported in 24-bit TIFF format. For illustrating purpose, the red, green, and blue channels were subsequently separated from original picture with Adobe Photoshop® 7.0 software.

Determination of LPS within the brain parenchyma

Brain sections from the first and second groups of mice treated or not with either DFMO (2% in drinking water) or LPS i.p. (1 mg/kg body weight) were washed in KPBS and incubated for 3 h at 37°C with KPBS containing 10% goat serum. Additional tissues from animals that received a single bolus of LPS into the dorsal basal ganglia were used as positive controls. Tissues were thereafter rinsed in KPBS and incubated for 16 h at 4°C with anti-lipid A antibody (clone 43, lot HM 2046–3422 M11; Cell Sciences), which was diluted in sterile KPBS (1:1,000) plus 0.4% Triton X-100 and 1% BSA (fraction V; Sigma-Aldrich). Brain slices were subsequently rinsed in KPBS and incubated with a mixture of KPBS plus 0.02% Triton X-100,

1% BSA, and Alexa Fluor® 488 goat anti–mouse IgG Ab (1:1,500; Molecular Probes, Inc.) for 3 h at 20°C. Tissues were thereafter rinsed in KPBS. Photomicrographs were taken with the same exposure time (9 s) using a digital camera (SPOT RT Slider; Diagnostic Instruments) mounted directly on a microscope (BX-60; Olympus) equipped with an FITC-specific epifluorescence filter and connected to a Macintosh computer (Power Macintosh G4; Apple Computers).

Qualitative analysis

The relative intensity of TLR2 or TNF-α mRNA signals throughout the brain of each animal was assessed on dipped emulsion slides under microscopic evaluation, and was graded according to the scale of undetectable (0), low (1), moderate (2), strong (3), or very strong (4) signal.

Quantitative analysis

Semi-quantitative analysis of the TLR2 and TNF-α mRNA hybridization signal was performed on nuclear emulsion–dipped slides with a CCD video camera (Sony) attached to a Bmax optical system (BX-50; Olympus) coupled to a computer. The refractory density in arbitrary unit (RDAU) of the hybridization signal was measured under darkfield illumination at a magnification of 25 using NIH Image software (version 1.61 for Macintosh PPC; Wayne Rasband, National Institutes of Health, Bethesda, MD). The RDAUs of regions of interest were then corrected for the average background signal by sampling cells immediately outside the region of interest without positive hybridization signal. Data are reported as a percentage of control (vehicle i.p., vehicle i.c.v.) of mean RDAU values (± SEM). Statistical analysis was performed by ANOVA, followed by a Bonferroni/Dunn test procedure as post-hoc comparisons with Statview software (version 4.01, Macintosh).

References

Auvinen, M., A. Paasinen, L.C. Andersson, and E. Holtta. 1992. Ornithine decarboxylase activity is critical for cell transformation. *Nature.* 360:355–358.

Bey, P., C. Danzin, V. Van Dorsselaer, P. Mamont, M. Jung, and C. Tardif. 1978. Analogues of ornithine as inhibitors of ornithine decarboxylase. New deductions concerning the topography of the enzyme's active site. *J. Med. Chem.* 21:50–55.

Bradford, M.M. 1976. A rapid and sensitive method for the quantitation of microgram quantities of protein utilizing the principle of protein-dye binding. *Anal. Biochem.* 72:248–254.

Cai, D., K. Deng, W. Mellado, J. Lee, R.R. Ratan, and M.T. Filbin. 2002. Arginase I and polyamines act downstream from cyclic AMP in overcoming inhibition of axonal growth MAG and myelin in vitro. *Neuron.* 35:711–719.

Clarke, J.R., and A.S. Tyms. 1991. Polyamine biosynthesis in cells infected with different clinical isolates of human cytomegalovirus. *J. Med. Virol.* 34:212–216.

de Vries, H.E., E.F. Eppens, M. Prins, J. Kuiper, T.J. van Berkel, A.G. de Boer, and D.D. Breimer. 1995. Transport of a hydrophilic compound into the

cerebrospinal fluid during experimental allergic encephalomyelitis and after lipopolysaccharide administration. *Pharm. Res.* 12:1932–1936.

Dyatlov, V.A., A.V. Platoshin, D.A. Lawrence, and D.O. Carpenter. 1998. Lead potentiates cytokine- and glutamate-mediated increases in permeability of the blood-brain barrier. *Neurotoxicology.* 19:283–291.

Fakler, B., U. Brandle, E. Glowatzki, S. Weidemann, H.P. Zenner, and J.P. Ruppersberg. 1995. Strong voltage-dependent inward rectification of inward rectifier K$^+$ channels is caused by intracellular spermine. *Cell.* 80:149–154.

Ficker, E., M. Taglialatela, B.A. Wible, C.M. Henley, and A.M. Brown. 1994. Spermine and spermidine as gating molecules for inward rectifier K$^+$ channels. *Science.* 266:1068–1072.

Fozard, J.R., M.L. Part, N.J. Prakash, J. Grove, P.J. Schechter, A. Sjoersma, and J. Koch-Weser. 1980. L-Ornithine decarboxylase: an essential role in early mammalian embryogenesis. *Science.* 208:505–508.

Gilad, G.M., and V.H. Gilad. 1988. Early polyamine treatment enhances survival of sympathetic neurons after postnatal axonal injury or immunosympathectomy. *Brain Res.* 466:175–181.

Gilad, G.M., and V.H. Gilad. 2002. Stress-induced dynamic changes in mouse brain polyamines. Role in behavioral reactivity. *Brain Res.* 943:23–29.

Ha, H.C., N.S. Sirisoma, P. Kuppusamy, J.L. Zweier, P.M. Woster, and R.A. Casero, Jr. 1998. The natural polyamine spermine functions directly as a free radical scavenger. *Proc. Natl. Acad. Sci. USA.* 95:11140–11145.

Hasko, G., D.G. Kuhel, A. Marton, Z.H. Nemeth, E.A. Deitch, and C. Szabo. 2000. Spermine differentially regulates the production of interleukin-12 p40 and interleukin-10 and suppresses the release of the T helper 1 cytokine interferon-gamma. *Shock.* 14:144–149.

Hillary, R.A., and A.E. Pegg. 2003. Decarboxylases involved in polyamine biosynthesis and their inactivation by nitric oxide. *Biochim. Biophys. Acta.* 1647:161–166.

Janne, J., and H.G. Williams-Ashman. 1971. On the purification of L-ornithine decarboxylase from rat prostate and effects of thiol compounds on the enzyme. *J. Biol. Chem.* 246:1725–1732.

Katz, A., and C. Kahana. 1987. Transcriptional activation of mammalian ornithine decarboxylase during stimulated growth. *Mol. Cell. Biol.* 7:2641–2643.

Kilpelainen, P., E. Rybnikova, O. Hietala, and M. Pelto-Huikko. 2000. Expression of ODC and its regulatory protein antizyme in the adult rat brain. *J. Neurosci. Res.* 62:675–685.

Kilpelainen, P.T., J. Saarimies, S.I. Kontusaari, M.J. Jarvinen, A.P. Soler, M.J. Kallioinen, and O.A. Hietala. 2001. Abnormal ornithine decarboxylase activity in transgenic mice increases tumor formation and infertility. *Int. J. Biochem. Cell Biol.* 33:507–520.

Laflamme, N., and S. Rivest. 2001. Toll-like receptor 4: the missing link of the cerebral innate immune response triggered by circulating gram-negative bacterial cell wall components. *FASEB J.* 15:155–163.

Laflamme, N., S. Lacroix, and S. Rivest. 1999. An essential role of interleukin-1β in mediating NF-κB activity and COX-2 transcription in cells of the blood-brain barrier in response to a systemic and localized inflammation but not during endotoxemia. *J. Neurosci.* 19:10923–10930.

Laflamme, N., G. Soucy, and S. Rivest. 2001. Circulating cell wall components derived from gram-negative, not gram-positive, bacteria cause a profound induction of the gene-encoding toll-like receptor 2 in the CNS. *J. Neurochem.* 79:648–657.

Lopatin, A.N., E.N. Makhina, and C.G. Nichols. 1994. Potassium channel block by cytoplasmic polyamines as the mechanism of intrinsic rectification. *Nature.* 372:366–369.

Lustig, S., H.D. Danenberg, Y. Kafri, D. Kobiler, and D. Ben-Nathan. 1992. Viral neuroinvasion and encephalitis induced by lipopolysaccharide and its mediators. *J. Exp. Med.* 176:707–712.

Marchetti, B., R. Poulin, M. Plante, and F. Labrie. 1988. Castration levels of plasma testosterone have potent stimulatory effects on androgen-sensitive parameters in the rat prostate. *J. Steroid Biochem.* 31:411–419.

Matsufuji, S., T. Matsufuji, Y. Miyazaki, Y. Murakami, J.F. Atkins, R.F. Gesteland, and S. Hayashi. 1995. Autoregulatory frameshifting in decoding mammalian ornithine decarboxylase antizyme. *Cell.* 80:51–60.

McKay, L.I., and J.A. Cidlowski. 1999. Molecular control of immune/inflammatory responses: interactions between nuclear factor-kappa B and steroid receptor-signaling pathways. *Endocr. Rev.* 20:435–459.

Messina, L., A. Arcidiacono, G. Spampinato, L. Malaguarnera, G. Berton, L. Kaczmarek, and A. Messina. 1990. Accumulation of ornithine decarboxylase mRNA accompanies activation of human and mouse monocytes/macrophages. *FEBS Lett.* 268:32–34.

Meyskens, F.L., Jr., and E.W. Gerner. 1999. Development of difluoromethylornithine (DFMO) as a chemoprevention agent. *Clin. Cancer Res.* 5:945–951.

Morrison, L.D., X.C. Cao, and S.J. Kish. 1998. Ornithine decarboxylase in human brain: influence of aging, regional distribution, and Alzheimer's disease. *J. Neurochem.* 71:288–294.

Murakami, Y., S. Matsufuji, T. Kameji, S. Hayashi, K. Igarashi, T. Tamura, K. Tanaka, and A. Ichihara. 1992. Ornithine decarboxylase is degraded by the 26S proteasome without ubiquitination. *Nature.* 360:597–599.

Nadeau, S., and S. Rivest. 2000. Role of microglial-derived tumor necrosis factor in mediating CD14 transcription and nuclear factor kappa B activity in the brain during endotoxemia. *J. Neurosci.* 20:3456–3468.

Nadeau, S., and S. Rivest. 2001. The complement system is an integrated part of the natural innate immune response in the brain. *FASEB J.* 15:1410–1412.

Nadeau, S., and S. Rivest. 2002. Endotoxemia prevents the cerebral inflammatory wave induced by intraparenchymal lipopolysaccharide injection: role of glucocorticoids and CD14. *J. Immunol.* 169:3370–3381.

Nadeau, S., and S. Rivest. 2003. Glucocorticoids play a fundamental role in protecting the brain during innate immune response. *J. Neurosci.* In press.

Nguyen, M.D., J.P. Julien, and S. Rivest. 2002. Innate immunity: the missing link in neuroprotection and neurodegeneration? *Nat. Rev. Neurosci.* 3:216–227.

Nomura, F., S. Akashi, Y. Sakao, S. Sato, T. Kawai, M. Matsumoto, K. Nakanishi, M. Kimoto, K. Miyake, K. Takeda, and S. Akira. 2000. Cutting edge: endotoxin tolerance in mouse peritoneal macrophages correlates with down-regulation of surface toll-like receptor 4 expression. *J. Immunol.* 164:3476–3479.

Pegg, A.E., J.A. Secrist III, and R. Madhubala. 1988. Properties of L1210 cells resistant to alpha-difluoromethylornithine. *Cancer Res.* 48:2678–2682.

Persidsky, Y., M. Stins, D. Way, M.H. Witte, M. Weinand, K.S. Kim, P. Bock, H.E. Gendelman, and M. Fiala. 1997. A model for monocyte migration through the blood-brain barrier during HIV-1 encephalitis. *J. Immunol.* 158:3499–3510.

Porcella, A., C. Carter, D. Fage, C. Voltz, K.G. Lloyd, A. Serrano, and B. Scatton. 1991. The effects of N-methyl-D-aspartate and kainate lesions of the rat striatum on striatal ornithine decarboxylase activity and polyamine levels. *Brain Res.* 549:205–212.

Seiler, N. 2000. Oxidation of polyamines and brain injury. *Neurochem. Res.* 25:471–490.

Shimizu, H., Y. Kakimoto, and I. Sano. 1965. Changes in concentration of polyamines in the developing mouse brain. *Nature.* 207:1196–1197.

Szabo, C., G.J. Southan, E. Wood, C. Thiemermann, and J.R. Vane. 1994. Inhibition by spermine of the induction of nitric oxide synthase in J774.2 macrophages: requirement of a serum factor. *Br. J. Pharmacol.* 112:355–356.

Tabor, C.W., and H. Tabor. 1984. Polyamines. *Annu. Rev. Biochem.* 53:749–790.

Taveira da Silva, A.M., H.C. Kaulbach, F.S. Chuidian, D.R. Lambert, A.F. Suffredini, and R.L. Danner. 1993. Brief report: shock and multiple-organ dysfunction after self-administration of *Salmonella* endotoxin. *N. Engl. J. Med.* 328:1457–1460.

Tjandrawinata, R.R., L. Hawel III, and C.V. Byus. 1994. Regulation of putrescine export in lipopolysaccharide or IFN-gamma-activated murine monocytic-leukemic RAW 264 cells. *J. Immunol.* 152:3039–3052.

van Daalen Wetters, T., M. Macrae, M. Brabant, A. Sittler, and P. Coffino. 1989. Polyamine-mediated regulation of mouse ornithine decarboxylase is post-translational. *Mol. Cell. Biol.* 9:5484–5490.

White, M.W., T. Kameji, A.E. Pegg, and D.R. Morris. 1987. Increased efficiency of translation of ornithine decarboxylase mRNA in mitogen-activated lymphocytes. *Eur. J. Biochem.* 170:87–92.

Williams, K. 1997. Interactions of polyamines with ion channels. *Biochem. J.* 325:289–297.

Zhang, M., T. Caragine, H. Wang, P.S. Cohen, G. Botchkina, K. Soda, M. Bianchi, P. Ulrich, A. Cerami, B. Sherry, and K.J. Tracey. 1997. Spermine inhibits proinflammatory cytokine synthesis in human mononuclear cells: a counterregulatory mechanism that restrains the immune response. *J. Exp. Med.* 185:1759–1768.

Zhang, M., L.V. Borovikova, H. Wang, C. Metz, and K.J. Tracey. 1999. Spermine inhibition of monocyte activation and inflammation. *Mol. Med.* 5:595–605.

Zhang, M., H. Wang, and K.J. Tracey. 2000. Regulation of macrophage activation and inflammation by spermine: a new chapter in an old story. *Crit. Care Med.* 28:N60–N66.

Zheng, S.A., C.M. McElwain, and S.M. Taffet. 1991. Regulation of mouse ornithine decarboxylase gene expression in a macrophage-like cell line: synergistic induction by bacterial lipopolysaccharide and cAMP. *Biochem. Biophys. Res. Commun.* 175:48–54.